PARALLEL QUADRUPOLE BEAM-BASED ALIGNMENT FOR FCC-ee

C. Goffing*[1,2], J. Keintzel[1], A.-S. Müller[2], F. Zimmermann[1]
[1]CERN, Geneva, Switzerland
[2]Karlsruhe Institute of Technology, Karlsruhe, Germany

Abstract

The Future electron-positron Circular Collider (FCC-ee) is a proposed lepton collider for high-energy particle physics succeeding the High-Luminosity Large Hadron Collider (HL-LHC). Its ambitious design goals demand excellent orbit and optics control and, therefore, set strict limits on alignment tolerances. Beam-based alignment (BBA) is used to relax the mechanical alignment tolerances by determining the offset between the magnet and the measured beam position. Orbit correctors steer the particle beam towards the determined magnetic centre and thus reduce the effective quadrupole misalignment. A parallel BBA technique is compared for the Global Hybrid chromaticity Correction (GHC) and Local Chromaticity Correction (LCC) lattices for FCC-ee using Xsuite simulations.

INTRODUCTION

The Future electron-positron Circular Collider (FCC-ee) [1–3] is a proposed electroweak and Higgs factory succeeding the High-Luminosity Large Hadron Collider (HL-LHC) [4]. The centre-of-mass energy in the range from 91.2 GeV to 365 GeV allows the production of Z, W, Higgs bosons and top-antitop pairs [3]. Two conceptually different lattices have been developed, the so-called Global Hybrid chromaticity Correction (GHC) [5] and Local Chromaticity Correction (LCC) [6] lattices.

The ambitious luminosity target of 1.44×10^{36} cm^{-2} s^{-1} at 45.6 GeV [7], requires excellent orbit and optics control and implies strict boundaries on the accelerator optics and thus on alignment tolerances of all lattice elements. In particular, tight constraints apply for the maximum magnet misalignments and for the transverse offset of nearby beam-position monitor (BPM) readings from the centre of quadrupole and sextupole magnets in the range from 10 µm to 20 µm [7, 8]. With knowledge of the BPM reading corresponding to the magnetic centre, obtained through Beam-Based Alignment (BBA), the beam can be steered using orbit correctors to reduce the effective magnet misalignment.

The FCC-ee arcs contain about 85 % of the quadrupoles in the two lattices, arranged in magnet families to be powered in series. Due to the large number of magnets in the FCC-ee, not only a precise but also a fast method is required. A parallel BBA approach, which has been developed in recent years [9, 10] and simulated for earlier FCC-ee lattice versions [11, 12], is particularly suitable for this purpose. Similar schemes have been tested or used in various machines, including EBS at ESRF [13], SPEAR3 at SLAC [9], NSLS-II at BNL [14], KARA at KIT [15] and LHC at CERN [16].

* christian.goffing@cern.ch

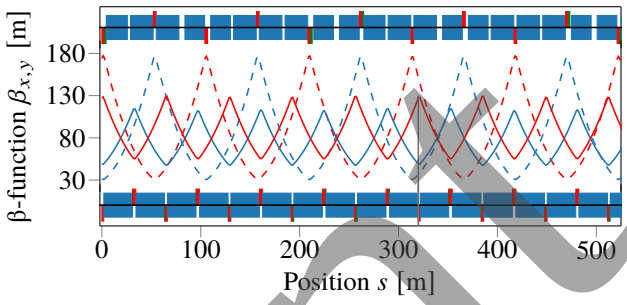

Figure 1: Arc lattice for GHC (upper lattice diagram, one supercell) and LCC (lower lattice diagram, first 320 m are one cell) as well as the horizontal (blue) and vertical (red) β-functions for GHC (dashed) and LCC (solid).

Table 1: Magnet Strength and Lengths of the Different Arc Quadrupole Families for the GHC and LCC Optics at Z

Quad family		Strength [T m^{-1}]		Length [m]	
GHC	LCC	GHC	LCC	GHC	LCC
QD1	QD1A	−1.56	−2.08	2.70	1.86
QF2	QF2A	1.56	1.41	2.70	2.89
QD3	QF3A	−1.56	1.43	2.70	2.89
QF4	QD1AM	1.56	−2.08	2.70	1.86

This paper compares a parallel BBA approach for the arc quadrupoles in the GHC and LCC optics at 45.6 GeV.

ARC LATTICES

For the comparison, the lattice versions 25.3 for GHC and 105 for LCC are considered [17]. In the arc sections, GHC features a FODO lattice with nearly identical quadrupole strengths and a phase advance of 90° per cell. Two different arc sections are used in the lattice, one comprising 89 FODO cells with the quadrupole families QD1 and QF2 and the other comprising 86 FODO cells with the quadrupole families QD3 and QF4. A supercell of the GHC lattice is made out of 10 quadrupole magnets or 5 FODO cells. LCC, on the other hand, is based on a uniform arc layout and a hybrid focusing defocusing (HFD) lattice. Ten quadrupole magnets, divided into 4 families, form a unit cell. The phase advance is significantly lower with 50° (44°) in the horizontal (vertical) plane between two consecutive (de)focusing quadrupoles. Each of the eight arc sections consists of 27 cells. The magnet layout and beta functions are shown in Fig. 1, and the parameters for the arc quadrupoles in Table 1.

BBA TECHNIQUES

A centred beam experiences only the desired focusing upon its passage through an ideal quadrupole. However, if

Table 2: Magnet Misalignment and Field Errors in Arcs and Technical Straights (TS)

Element	$\sigma_{x,y}$ [µm]	σ_θ [µrad]	σ_z [µm]	$\Delta k/k$ [10^{-4}]
Arc quads & sexts*	50	50	100	2
Girder	150	150	500	-
Arc Dipoles	1000	1000	500	10
BPM-to-quad	100	10	-	-
TS quads & sexts	50	50	100	2
TS Dipoles	1000	1000	100	10

* Misalignment relative to girder

the beam is transversely offset relative to the magnetic centre, the beam experiences an additional dipole component, causing a centroid deflection of the beam. This deflection is proportional to the beam offset and to the quadrupole strength. Therefore, the deflection varies when the magnet strength is changed [12, Eq. (1)]. In the BBA approach presented here, the strength of an orbit corrector close to the quadrupole is adjusted to compensate for the kick strength change due to the modulated quadrupole so as to keep the closed orbit constant. The beam offset in the magnet is inferred from the proportionality factor relating the quadrupole and dipole components. Thus, the ratio of the changes in the dipole field, here obtained through the integral corrector strength, and in the quadrupole strength yields the beam offset relative to the magnetic centre of the magnet. With additional beam position measurements next to the quadrupole, the BPM-to-quadrupole offset is determined.

SIMULATION SETTINGS

For the simulations, BPMs and vertical orbit correctors are attached to the end of each quadrupole. Horizontal orbit correctors are also located at the quadrupoles in the technical straights and interaction region, while in the arcs, the horizontal correctors are attached to the bending magnets adjacent to the quadrupoles. The nominal collision optics for both lattices at Z energy are used. Since for the real machine, the BBA is intended to be part of the accelerator commissioning, with interaction-region quadrupoles switched off [7,8], in our "pseudo-ballistic" model setup only the magnets of the arcs and the technical straights are misaligned in all three directions and rotated around the beam axis, according to the errors specified in Table 2. The σ values of the table represent one standard deviation for a Gaussian distribution truncated at 2.5 σ.

In a first step, misalignment and field errors are introduced for the magnets in the Xsuite [18] simulation, before a closed orbit is sought using threading and orbit correction. When correcting the orbit, an uncertainty of 1 µm is taken into account for the closed orbit measurement. In the next step, a BPM to quadrupole misalignment of 100 µm is added. Starting from 100 seeds, for the LCC optics with 10 seeds no closed orbit is found after the complete misalignment, whereas all seeds succeed for GHC. The failed seeds exhibit

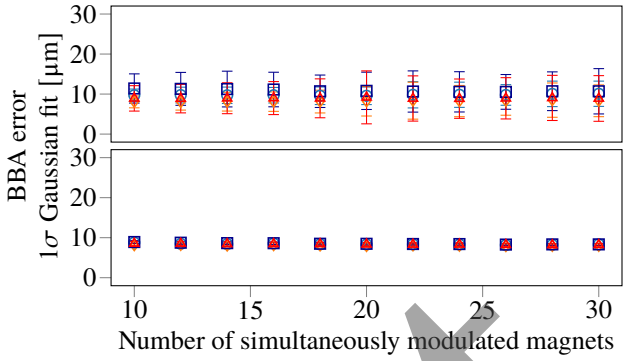

Figure 2: Dependence of rms BBA accuracy on number of simultaneously modulated quadrupoles for GHC (upper plot) and LCC (lower plot). The results for BBA with the same quadrupole strength change are shown in light blue (horizontal) and orange (vertical), and similarly for alternating k in dark blue (horizontal) and red (vertical).

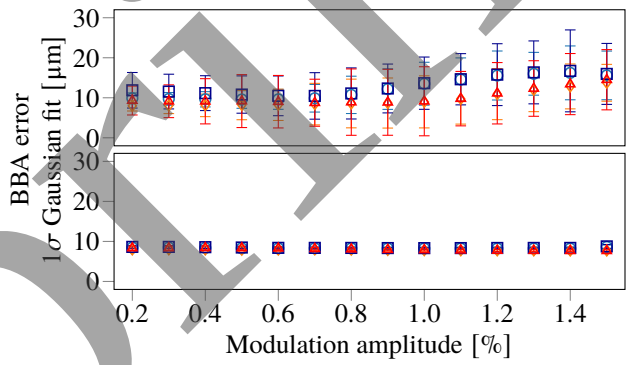

Figure 3: Dependence of rms BBA accuracy on modulation amplitude for GHC (upper plot) and LCC (lower plot). The results for BBA with the same quadrupole strength change are shown in light blue (horizontal) and orange (vertical), and similarly for alternating k in dark blue (horizontal) and red (vertical).

numerical instabilities in the threading, depending on the chosen parameters. With different threading parameters, a closed orbit can also be found for these failed seeds [19]. Subsequently, a group of consecutive magnets of a family is selected for the BBA. The BBA step is repeated until it has been performed for all the arc quadrupoles. Both the number of modulated magnets and the modulation amplitude are varied in the simulations. The strength of consecutive magnets of a family is changed either by the same or by the opposite value, i.e., with an increase for one magnet and a reduction for the next.

BBA RESULTS

For the comparison of BBA for LCC and GHC, the simulations are performed with comparable settings. The number of simultaneously modulated magnets is varied in the range from 10 to 30 magnets, while a constant modulation amplitude of 0.5 % is used. The results are presented in Fig. 2. No dependence on the number of magnets is observed for either of the two lattices and any of the BBA methods considered.

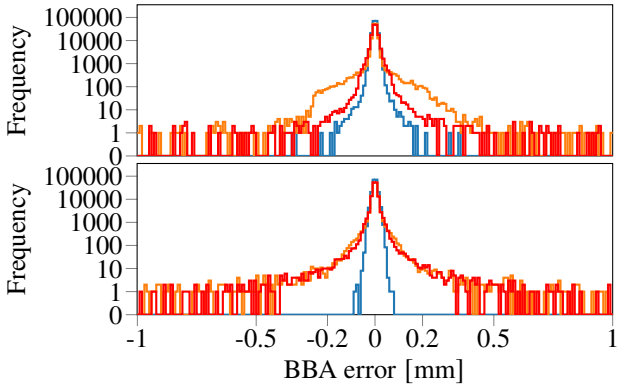

Figure 4: Frequency of horizontal (upper plot) and vertical BBA errors (lower plot) over all seeds for LCC (blue) and for GHC with both the original (orange) and the modified placement of BPM and corrector (red).

Previous simulations have shown that the residual BBA errors remain constant for up to around 30 quadrupoles and increase for higher numbers of magnets [12]. When varying the modulation amplitude in the range from 0.2 % to 1.5 %, as shown in Fig. 3, a constant number of 20 magnets is modulated. For the LCC BBA, using the same relative change in k for all magnets, the error is constant for the parameter range under consideration. The BBA with alternating quadrupole strength changes shows similar but up to 0.4 µm larger errors. The GHC BBA, on the other hand, favours smaller modulation amplitudes, below 0.7 % to 1.0 %. For larger amplitudes, the deviations increase. For GHC, the BBA errors in the vertical plane are slightly smaller than in the horizontal plane. The deviations for the BBA with alternating quadrupole strengths are up to 2 µm higher.

The BBA error is defined here as the absolute error between the calculated and the set magnetic offset. For each seed, the values are displayed as a histogram and the width of the distribution is determined using a Gaussian fit. The mean value and standard deviation of the individual seeds are entered as data points and error bars in the plot. In GHC, approximately 1.7 % of outliers with an error above 50 µm are observed. Especially large values significantly increase the rms value, and hence a Gaussian fit is used here. The percentage of outliers for the BBA at the LCC is smaller than 1.4 ‰. For most of the data points, the difference between the fit and the rms value lies between 1 µm and 5 µm with a maximal difference of 15 µm. The distribution of outliers for LCC and GHC with differences in BPM and corrector placement is displayed in Fig. 4. One explanation for the poorer reproducibility in GHC is a phase advance of exactly 90° per FODO cell in this arc, which translates into a systematic degeneracy in the orbit response matrix. The resulting harmonic correlation between corrector response vectors reduces the effective matrix rank and deteriorates its conditioning, thereby limiting the robustness of orbit correction and optics reconstruction. In the horizontal plane, the outliers with absolute deviations in the range from 60 µm to 300 µm are reduced if the phase advance between BPMs

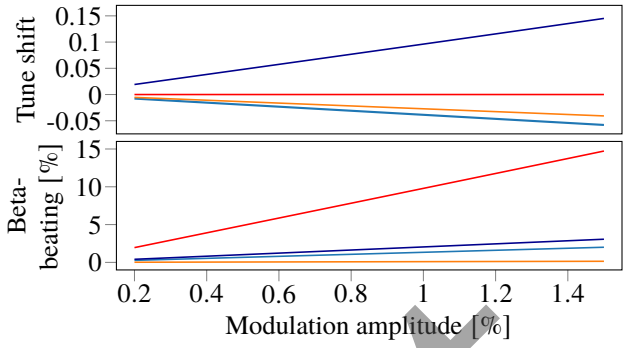

Figure 5: Horizontal tune shift (upper plot) and beta-beating (lower plot) for QD1 family for modulation for normal BBA in LCC (light blue) and GHC (orange). For alternating k, it is shown in dark blue for LCC and red for GHC.

and correctors is not exactly 45° between two subsequent quadrupoles, but fluctuates slightly around this value. This is achieved by placing the BPMs and correctors partly before and partly after the quadrupoles in GHC [19].

However, the phase advance of 90° per FODO cell and thus between modulated magnets in the GHC lattice allows the reduction of beta-beating when using the same change in quadrupole strength or tune shifts for alternating k. The dependence of the tune shift and beta-beating on the modulation amplitude for 20 simultaneously modulated magnets of the QD1(A) family is shown in Fig. 5. This same intrinsic compensation does not apply for the LCC optics, leading to comparably high beta-beating and tune shift for the alternating k values. For GHC, both variants appear suitable for the BBA: changing subsequent quadrupole strengths by the same value or by an alternating value here leads to a comparable error. In this way, either the tune shift caused by modulation or the beta-beating are minimised. For LCC, changing by the same value appears superior, as both beta-beating and tune shift are smaller in this variant.

SUMMARY AND OUTLOOK

The simulated parallel quadrupole BBA yields comparable accuracies for the FCC-ee GHC and LCC lattices. The target BBA accuracy of 10 µm to 20 µm, therefore, appears feasible. Both lattices allow the simultaneous offset determination for 10 to 30 magnets. The LCC favors larger modulation amplitudes, the GHC smaller ones. Much larger outliers are found for the GHC lattice and these significantly contribute to the rms BBA error.

In future simulations, the impact of larger BPM tilts, ground motion, long-range misalignment and shifts in the magnetic centre during modulation on BBA accuracy will be examined. In addition, we plan to simulate a complete commissioning sequence with both BBA and optics corrections [7, 8]. Starting from a ballistic optics and arc corrections, we will proceed through various relaxed optics with decreasing β^*, applying BBA and optics corrections in the interaction region, to ultimately arrive at the collision optics with nominal β^*.

REFERENCES

[1] M. Benedikt, A. Blondel, P. Janot, M. Mangano, and F. Zimmermann, "Future Circular Colliders succeeding the LHC", *Nat. Phys.*, vol. 16, no. 4, pp. 402–407, 2020. doi:10.1038/s41567-020-0856-2

[2] F. Zimmermann, M. Benedikt, K. Oide, and T. Raubenheimer, "The Electron-Positron Future Circular Collider (FCC-ee)", in *Proc. 5th Int. Particle Accel. Conf. (NAPAC'22)*, Albuquerque, NM, USA, Aug. 2022, pp. 315–320. doi:10.18429/JACoW-NAPAC2022-TUZD1

[3] M. Benedikt *et al.*, "Future Circular Collider Feasibility Study Report", CERN, Geneva, Rep. 12, 2025. doi:10.17181/CERN.9DKX.TDH9

[4] G. Apollinari *et al.*, Eds., "High-Luminosity Large Hadron Collider (HL-LHC): Technical design report", Geneva, 2020, doi:10.23731/CYRM-2020-0010,

[5] K. Oide *et al.*, "Design of beam optics for the future circular collider e^+e^- collider rings", *Phys. Rev. Accel. Beams*, vol. 19, no. 11, p. 111005, Nov. 2016. doi:10.1103/PhysRevAccelBeams.19.111005

[6] P. Raimondi, S. M. Liuzzo, L. Farvacque, S. White, and M. Hofer, "Local chromatic correction optics for Future Circular Collider e^+e^-", *Phys. Rev. Accel. Beams*, vol. 28, no. 2, p. 021002, Feb. 2025. doi:10.1103/PhysRevAccelBeams.28.021002

[7] M. Benedikt *et al.*, "Future Circular Collider Feasibility Study Report Volume 2: Accelerators, technical infrastructure and safety", CERN, Geneva, Switzerland, Rep. CERN-FCC-ACC-2025-0004, 2025. doi:10.17181/CERN.EBAY.7W4X

[8] R. Tomás *et al.*, "Optics tuning of the FCC-ee", in *Proc. IPAC'25*, Taipei, Taiwan, May 2025, pp. 282–285, Jun. 2025. doi:10.18429/JACoW-IPAC2025-MOPM009

[9] X. Huang, "Simultaneous beam-based alignment measurement for multiple magnets by correcting induced orbit shift", *Phys. Rev. Accel. Beams*, vol. 25, no. 5, p. 052802, May 2022. doi:10.1103/PhysRevAccelBeams.25.052802

[10] X. Huang, "Parallel quadrupole modulation for fast beam-based determination of magnet centers", in *Proc. IPAC'24*, Nashville, TN, USA, May 2024, pp. 3341–3344. doi:10.18429/JACoW-IPAC2024-THPG37

[11] X. Huang, "Beam-based alignment simulations for the Future Circular Collider electron lattice", in *Proc. IPAC'24*, Nashville, TN, USA, May 2024, pp. 308–311. doi:10.18429/JACoW-IPAC2024-MOPG08

[12] C. Goffing, J. Keintzel, A.-S. Müller, M. Reissig, and F. Zimmermann, "Beam-based alignment techniques for the fcc-ee", in *Proc. IPAC'25*, Taipei, Taiwan, May 2025, pp. 571–574, Jun. 2025. doi:10.18429/JACoW-IPAC2025-MOPM109

[13] S. Liuzzo, L. Carver, L. Valle, N. Carmignani, S. White, and T. Perron, "Parallel beam-based alignment for the EBS storage ring", in *Proc. IPAC'24*, Nashville, TN, USA, May 2024, pp. 1278–1281. doi:10.18429/JACoW-IPAC2024-TUPG27

[14] M. Song, X. Yang, J. Choi, Y. Hidaka, X. Huang, and G. Wang, "Test of parallel beam-based alignment at NSLS-II", in *Proc. IPAC'24*, Nashville, TN, USA, May 2024, pp. 3237–3239. doi:10.18429/JACoW-IPAC2024-THPC83

[15] C. Goffing *et al.*, "Experimental validation of parallel quadrupole beam-based alignment at KARA", *Journal of Physics: Conference Series*, vol. 3094, no. 1, p. 012041, Sep. 2025. doi:10.1088/1742-6596/3094/1/012041

[16] C. Goffing, M. Hostettler, J. Keintzel, A.-S. Müller, and J. Wenninger, "First Parallel Arc Quadrupole Beam-Based Alignment Using K-Modulation at LHC", presented at IPAC'26, Deauville, France, May 2026, paper WEP5035, this conference,

[17] CERN Optics Repository, Future Circular Collider optics repository, `https://gitlab.cern.ch/acc-models/fcc/acc-models-fcc-ee`

[18] G. Iadarola *et al.*, "Xsuite: an integrated beam physics simulation framework", in *Proc. HB'23*, Geneva, Switzerland, Oct. 2023, pp. 73–80, 2023. doi:10.18429/JACoW-HB2023-TUA2I1

[19] C. Goffing, News on beam-based alignment, Sep. 2024, `https://indico.cern.ch/event/1675106/contributions/7041742/attachments/3257887/5815860/20260417_BBA_Tuning_Meeting.pdf`